Supplementary information of

Synthesis, crystal structure and characterization of novel open-framework CHA-type aluminophosphate involving a chiral diamine

Kenichi KOMURA[1], Yukiko HORIBE[1], Hiroaki YAJIMA[1], Norihito HIYOSHI[2], and Takuji IKEDA[2,*]

[1] *Department of Materials Science and Technology, Faculty of Engineering, Gifu University, Yanagido 1-1, Gifu, 501-1193, Japan.*

[2] *Research Institute for Chemical Process Technology, National Institute of Advanced Industrial and Science and Technology, Nigatake 4-2-1, Sendai, 983-8551, Japan*
* corresponding author

CORRESPONDING AUTHOR FOOTNOTE: Takuji IKEDA, AIST Tohoku, 4-2-1, Nigatake, Miyagino-ku, Sendai 983-8551, JAPAN, TEL: +81-22-237-3013, FAX: +81-22-237-7027, E-mail: takuji-ikeda@aist.go.jp

1. Elementary analysis of GAM-1

Chemical analysis was carried out by using energy-dispersive X-ray spectrometry (EDX) by using BrukerAXS Quantax XFlash® 6|100 system. The EDX detector is equipped with FE-SEM (Hitachi S-4800). The existence of F element was detected in as-synthesized GAM-1 (Fig. S1(b)), although GAM-1 was synthesized without using a fluorine source at all. Empirical Al:P:F ratio was roughly estimated as 1.0:1.0:0.3. The signal attributed to F element was disappeared after calcination completely (Fig. S1(d)).
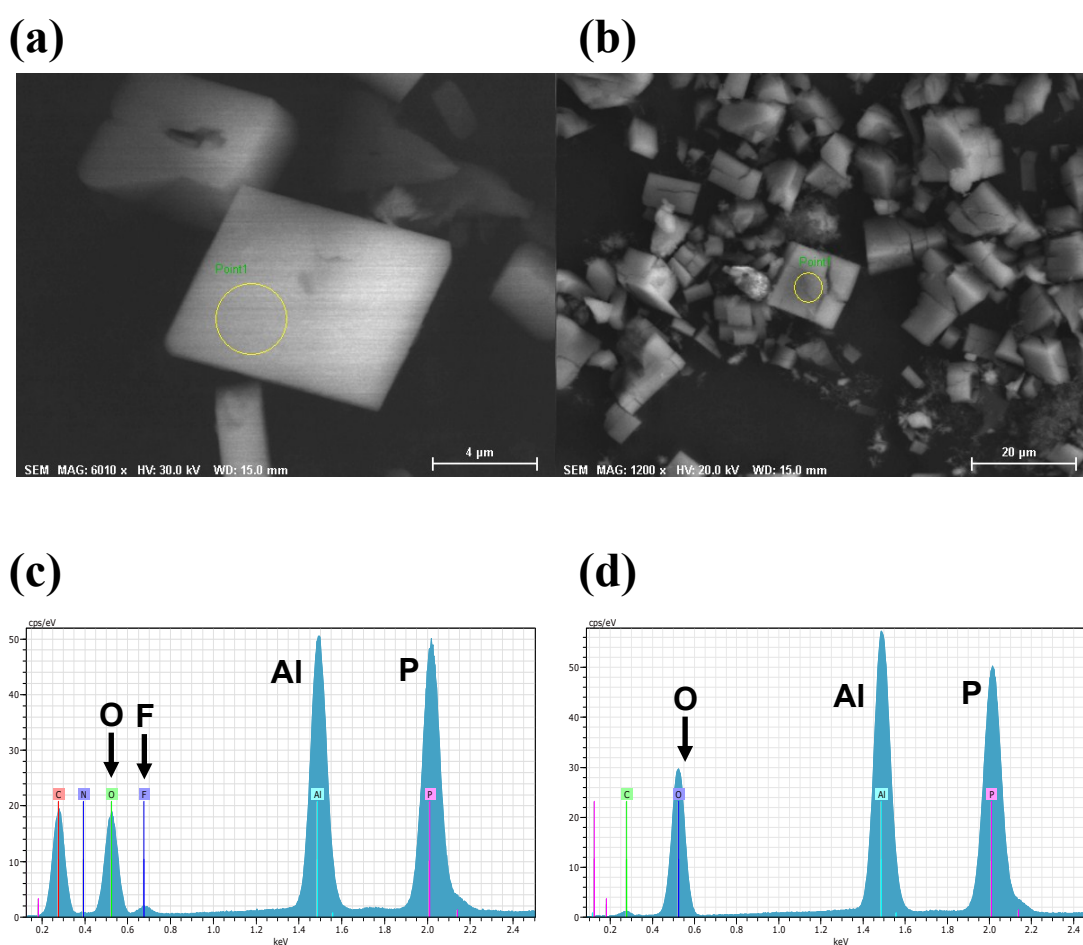
Figure S1. Upper figures show the SEM image of (a) GAM-1 and (b) calcined GAM-1. Yellow open circle shows the EDX analysis area. Lower figures show the EDX spectra of (c) GAM-1 and (d) calcined GAM-1.

2. Structural change of GAM-1 to AlPO$_4$-34 by calcination elucidated by high-temperature PXRD

A structural change by elevated temperature was confirmed by the HT-PXRD measurement. The diffraction peaks of GAM-1 (triclinic phase) were changed to those of the calcined-dehydrated form of AlPO$_4$-34 by the elevated temperature up to 400°C (Figure S1). This result consists with the monotonically weight loss in TG-DTA measurement due to the dehydration vide supra. At high-temperature, the observed PXRD pattern coincides with that of the rhombohedral **CHA**-type structure. In Figure S1, a generation of a small amount of unknown dense phase (indicated by arrows) was identified, which would be due to incomplete combustion of OSDA without enough air in narrow capillary tube and destruction of crystalline surface. The rhombohedral AlPO$_4$-34 was transformed into a triclinic structure (typical AlPO$_4$-34) again by rehydration at room temperature (Figure S2).
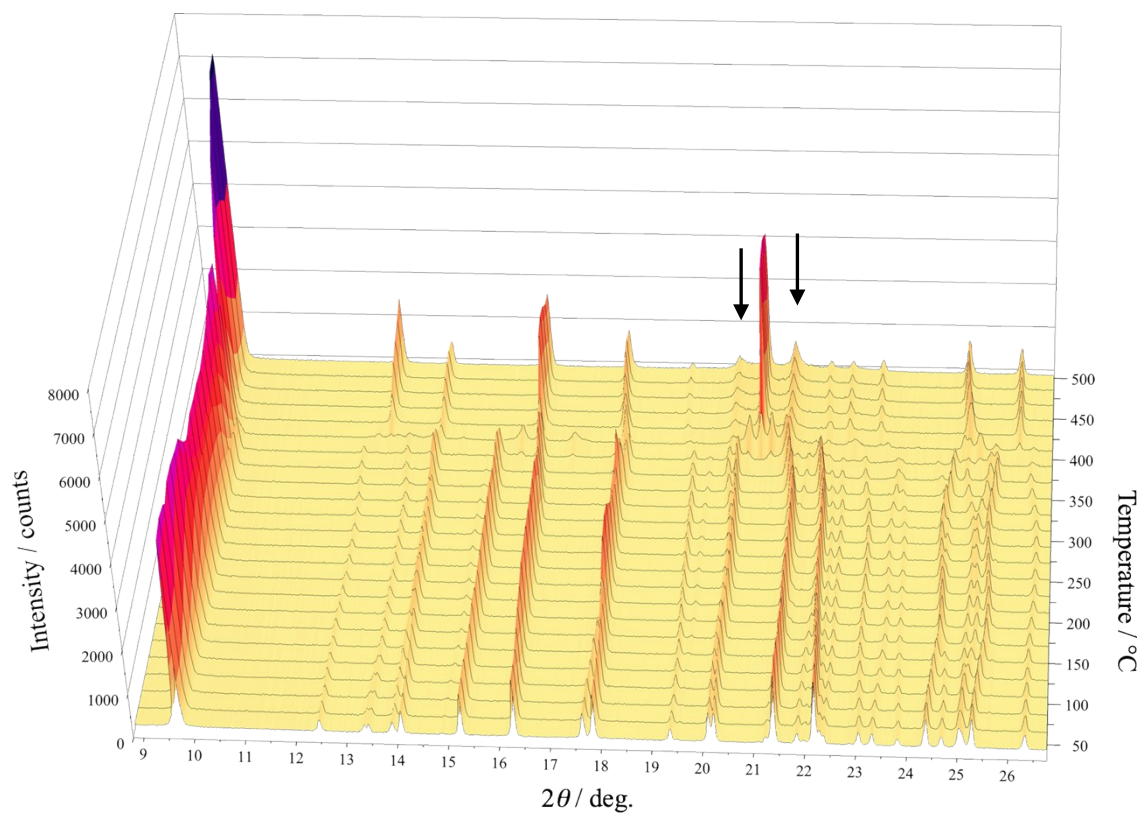
Figure S2. Bird's-eye view of HT-PXRD diagram of GAM-1. Arrows indicate the

presence of unknown dense phase observed over 400°C.
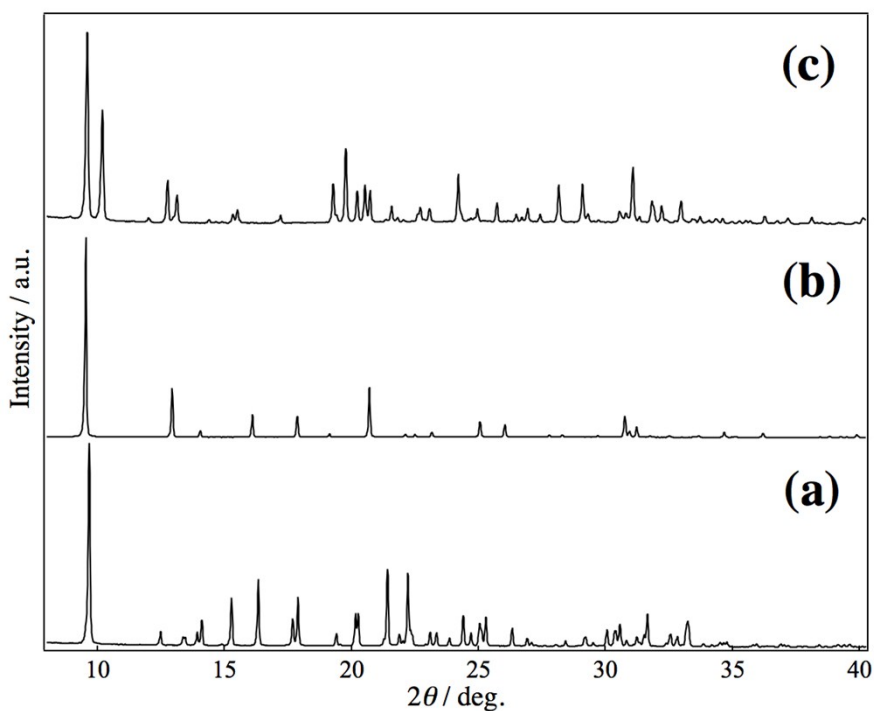
Figure S3. PXRD patterns of (a) as-synthesized GAM-1 measured at R.T., (b) calcined and dehydrated GAM-1 measured at 250°C and (c) after rehydration of (b) measured at R.T. In (b) and (c), lattice constants were $a = 13.6874(3)$ Å and $c = 14.8979(3)$ Å with space group $R\bar{3}$ (The setting of hexagonal axis was applied.), and $a = 8.9998(4)$ Å, $b = 9.2716(4)$ Å, $c = 9.5683(5)$ Å, $\alpha = 95.129(2)°$, $\beta = 104.742(2)°$ and $\gamma = 95.619(2)°$ with space group $P1$.

3. Liquid and solid-states ^{15}N NMR spectra of OSDA(1) and GMA-1.
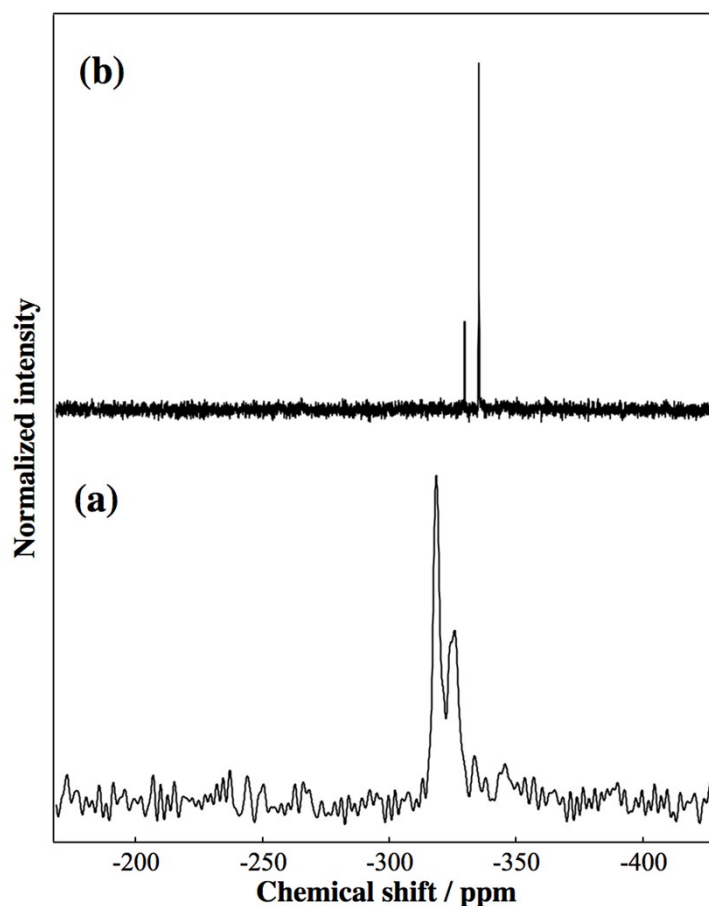
Figure S4. (a) $\{^1H\}$-^{15}N CP/MAS spectra of GAM-1 and (b) ^{15}N NMR spectra of OSDA (**1**) in CDCl$_3$ solvent. (a) shows two resonance peak at −318.5 ppm and −325.6 ppm, and (b) also shows two resonance peak at −329.55 ppm and −335.20 ppm. Chemical shifts of both spectra were converted on the basis of the standard reference value of CH$_3$NO$_2$ (0 ppm). In (a), contact time was set at 500 μs and a recycle delay of scan was 5 sec. The cumulated number of scan was over 150,000 times (ca. 8.6 day).

4. ^{27}Al 3QMAS NMR spectrum of GAM-1.

To clarify the number of independent Al site, ^{27}Al 3QMAS NMR spectrum with z-filter was also measured with {^{1}H} decoupling and rotor spinning rate of 24 kHz using an AVANCEIII 400WB spectrometer (Bruker Biospin K.K., Japan) and using a 3.2 mm VT-MAS probe with zirconia rotor. Excitation and conversion pulse length were 5.4 us and 1.9 us, respectively. Selective pulse length was set at 26 us. Optimized ^{1}H decupling field was ca. 15 kHz. Obtained 2D spectrum (Figure S4) clearly show the presence of two resonance peaks of 4-coodinated Al nuclei in isotropic dimension (F1 axis), although broad two or three resonance peaks were observed around 38 ppm in MAS spectrum dimension (F2 axis). In AlO$_4$ resonance peaks, the peak shape is elongated along to F2 axis, indicating strong quadrupolar interaction.
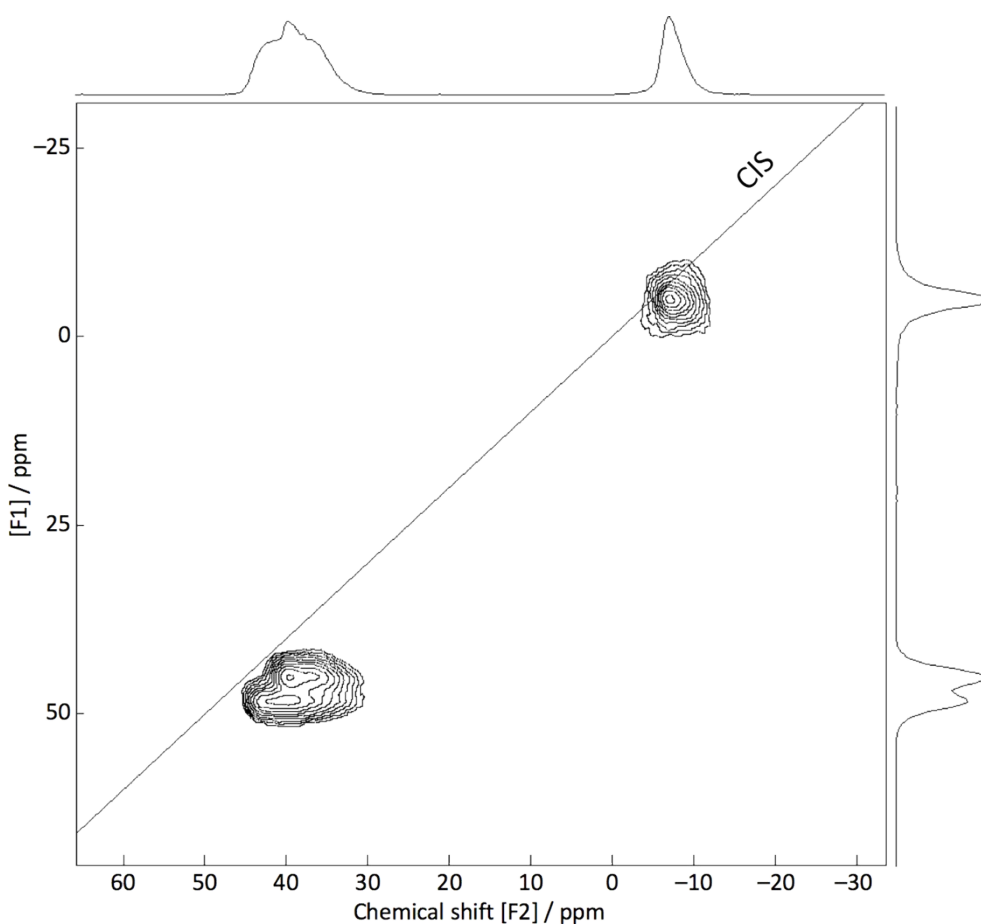
Figure S5. Sheared z-filtered ^{27}Al 3QMAS NMR spectrum for GAM-1.

7

5. Crystal structure analysis

High resolution powder XRD data of GAM-1 were collected at room temperature on a Bruker D8 Advance with Vαrio-1 diffractometer (Bruker AXS, Ltd., Japan) in modified Debye-Scherrer geometry. The sample was packed into a borosilicate glass capillary with an inner diameter of 0.5 mm. This diffractometer equipped with a wide range position-sensitive detector (VÅNTEC-1) and a Ge(111) primary monochromator yielding CuKα_1 radiation.

Structure analysis was carried out with the aid of the Rietveld method using the program RIETAN-FP [23]. Lattice constants were analyzed by indexing method using the program Rex.Cell [24]. Conformation and distribution of OSDA (**1**) in micropore was optimized by using the global optimization method with parallel tempering (PT) algorithm by using the program FOX [25]. In this analysis, Al, P and O atom positions were fixed at refined positions obtained by preliminary Rietveld analysis. Then, optimized conformation of OSDA or other guest molecules were introduced into structure refinement by the Rietveld method. Several iterative analyses between Rietveld analysis and PT optimization took place until R_{wp} value decreased to < 10 %. In this way, an initial structure model was constructed.

In the Rietveld analysis, the background was fitted using a combination of Legendre polynomial function with 11 coefficients and a prior background profile determined by spline interpolation. A split pseudo-Voigt function of Toraya with an asymmetry correction was used to model the profile shape. Partial profile relaxation with a modified split pseudo-Voigt function was applied in a low 2θ angle region, which significantly improved fits against strong asymmetric and/or anisotropic broadened profiles. The μr (μ: linear absorption coefficient, r: sample radius) values of the sample tubes was small, then there was no need to correct for X-ray absorption. During the early stage of refinement, we imposed restraints upon all of the T(Al or P)–(O or F) bond lengths and all the O–T–O and O–T–F bond angles. Furthermore, restraints were imposed upon all of the bond lengths and bond angles, which were based on the molecular geometry of OSDA (**1**), during structural refinement. Obtained structural models were visualized by using the program VESTA3 [26].
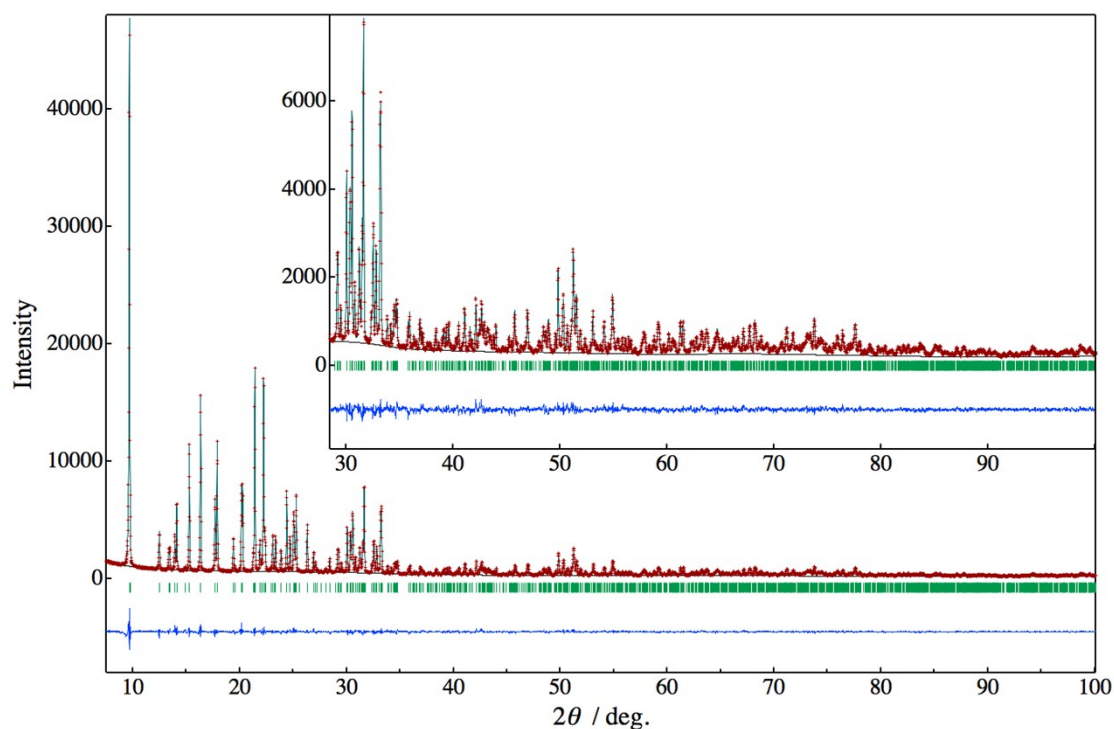
Figure S6. Observed pattern (red crosses), calculated pattern (light blue solid line), and difference pattern (blue) obtained by Rietveld refinement for GAM-1. The tick marks (green) denote the peak positions of possible Bragg reflections. The inset shows magnified patterns from 28.5° to 100°.

In the final refinement, three Al sites, three P sites, twelve O sites, two N site, nine C sites, 18 H site, three O_w sites, and six H_w sites were included in the asymmetric unit. All of the isotropic atomic displacement parameters, B, for the Al and P sites were constrained to be equal: $B(P_n) = B(Al_n)$ (n = 1~3). Simple approximations of $B(O1) = B(O_m: m = 2~12) = B(F)$ and $B(C) = B(N) = B(H)$ and $B(O_w) = B(H_w)$ were also imposed on the B parameters of all O sites, and all C, N, and H sites, and all O_w and H_w sites, respectively. The value of $B(O_w)$ was converged to 6.2 Å². Figure S6 shows difference plots obtained by the Rietveld analysis, indicating that our structural model is well agreement with observed data. Obtained R factors were sufficiently decreased to low levels, i.e., $R_{wp} = 5.7\%$ ($S = 1.63$), $R_F = 1.1\%$, and $R_{Bragg} = 1.6\%$.